Review Article

Raman Spectroscopic Studies on Two-Dimensional Materials

Jae-Ung Lee, Minjung Kim, Hyeonsik Cheong*

Department of Physics, Sogang University, Seoul 04107, Korea

*Correspondence to:
Cheong H,
Tel: +82-2-705-8434
Fax: +82-2-717-8434
E-mail: hcheong@sogang.ac.kr

Raman spectroscopy is one of the most widely used tools in the field of graphene and two-dimensional (2D) materials. It is used not only to characterize structural properties such as the number of layers, defect densities, strain, etc., but also to probe the electronic band structure and other electrical properties. As the field of 2D materials expanded beyond graphene to include new classes of layered materials including transition metal dichalcogenides such as MoS_2, new physical phenomena such as anomalous resonance behaviors are observed. In this review, recent results from Raman spectroscopic studies on 2D materials are summarized.

Key Words: Raman spectroscopy, Two-dimensional materials, Transition metal dichalcogenides

INTRODUCTION

Recently, two-dimensional (2D) materials attract much interest thanks to their unique physical properties and possible device applications. Graphene, a single atomic layer of graphite, is representative of 2D materials which have been studied intensively for about 10 years (Novoselov et al., 2004; Geim & Novoselov, 2007). Recently, the field has expanded to other layered materials, such as hexagonal boron nitride (Dean et al., 2010), transition metal dichalcogenides (TMDCs) (Mak et al., 2010; Wang et al., 2012), black phosphorus (Li et al., 2014; Liu et al., 2014), and so on. The physical properties of such layered materials vary greatly, from metals to semiconductors to insulators, and even some superconductors. In layered materials, each layer is weakly bonded by van der Waals interactions, and so the layers are easily exfoliated as shown in Fig. 1, which allows investigation of the properties of few-layer materials as opposed to bulk properties. In few-layer materials, the physical properties are strongly dependent on the number of layers since the interlayer interactions, albeit fairly small, play an important role in determining the band structure and other physical properties (Castro Neto et al., 2009). Therefore, identifying the number of layers has

been a key issue in studying these materials. Although various techniques have been used to identify the number of layers of the 2D materials, Raman spectroscopy remains one of the most widely used characterization methods (Ferrari & Basko, 2013). In this Review, we will summarize recent progress in Raman spectroscopy of graphene and other 2D materials.

DETERMINATION OF NUMBER OF LAYERS

In the case of graphene, the correlation between the Raman spectrum and the number of layers was established early on (Ferrari et al., 2006; Yoon et al., 2009a) and is still extensively used. The line shape of the so-called 2D band is strongly dependent on the number of layers, especially for 1 to 5 layers. More recently, this technique has expanded to identifying different stacking orders in graphene (Cong et al., 2011; Lui et al., 2011; Nguyen et al., 2014). Few-layer graphene can have two types of stacking, the usual Bernal or ABA stacking and rhombohedral or ABC stacking. The line shape of the 2D band depends not only on the number of layers, but also on the stacking order and the excitation energy of the laser used in the Raman measurement. By choosing appropriate excitation energies, one can unambiguously determine both
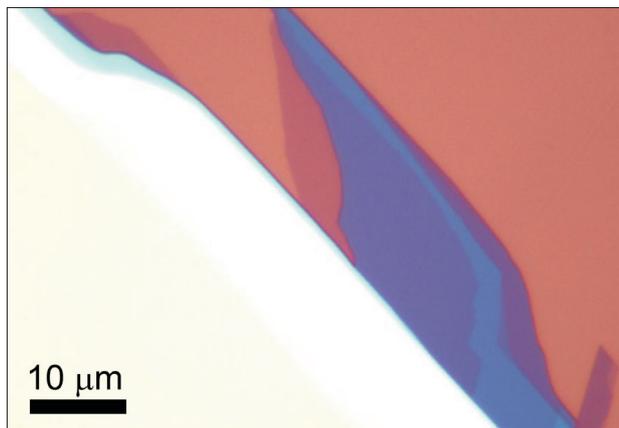
Fig. 1. Optical microscope image of a few-layer MoS$_2$ sample on a SiO$_2$/Si substrate.

Fig. 2. Raman spectra of 1 to 4-layer MoS$_2$ measured with the excitation energy of 2.41 eV. Vibrational modes are shown schematically.

the number of layers and the stacking order.

In the case of MoS$_2$, the most extensively studied among semiconducting TMDCs, the separation between the two main modes (E_{2g}^1 and A_{1g} modes) have been used to identify the number of layers (Lee et al., 2010). Fig. 2 shows typical Raman spectra of 1 to 4 layer MoS$_2$. The E_{2g}^1 mode corresponds to in-plane vibrations, and the A_{1g} mode to out-of-plane vibrations. The E_{2g}^1 mode redshifts as the number of layers increases whereas the A_{1g} mode blue shifts (Lee et al., 2010). The blue shift of A_{1g} mode with the number of layers can be explained by classical coupled harmonic oscillator, whereas the redshift of E_{2g}^1 with increasing number of layers has been attributed to the enhancement of dielectric screening of the long-range Coulomb interactions (Lee et al., 2010; Molina-Sánchez & Wirtz, 2011). Similar dependence of the E_{2g}^1 and A_{1g} modes on the number of layers has been observed for other semiconducting TMDCs such as MoSe$_2$ (Tonndorf et al., 2013; Chen et al., 2015), WS$_2$ (Zhao et al., 2013a; Chen et al., 2015), and WSe$_2$ (Luo et al., 2013; Zhao et al., 2013a; Chen et al., 2015). Furthermore, in MoSe$_2$ and WS$_2$, splitting of the A_{1g} mode has been observed (Tonndorf et al., 2013; Chen et al., 2015; Staiger et al., 2015). This splitting is known as the Davydov splitting due to interlayer interactions. Since the number of Raman active modes among such Davydov split modes and their frequencies depend on the number of layers, the number of layers can be reliably determined by monitoring the Davydov splitting (Tonndorf et al., 2013; Staiger et al., 2015). In the case of WSe$_2$, E_{2g}^1 and A_{1g} modes are closely overlapped and difficult to distinguish. Polarized Raman measurements can resolve this issue. Depending on the symmetry of vibrations, the polarization selection rule for each mode is different. By using linearly polarized light, the E_{2g}^1 mode can be observed for both parallel and cross polarization configurations, whereas the A_{1g} mode can be seen only in parallel polarization (Zhao et al., 2013b). A more
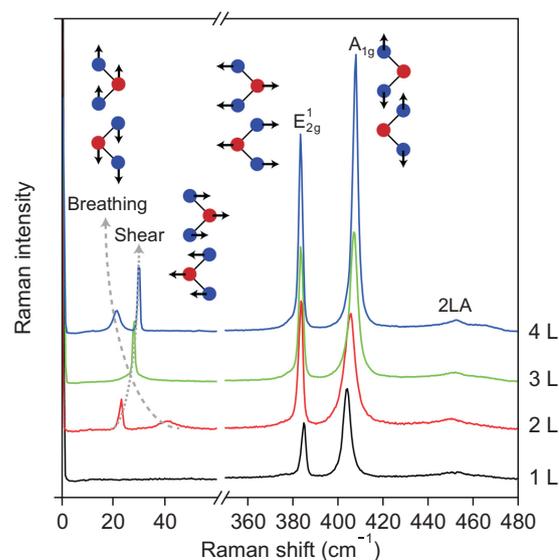
efficient way to distinguish these modes is using circularly polarized light. If the helicity of the incident and the scattered light is same, only the A_{1g} mode is observed, whereas only the E_{2g}^1 modes is observed with different helicity (Chen et al., 2015). This is an effective way to measure the frequency difference between these two modes especially for WSe$_2$.

Even though the main modes are good indicator of the number of layers, there are several limitations. Since the incremental shift gets smaller as the number of layers increases, this technique is limited to ~4 layers. In addition, because these modes are sensitive to other effects such as strain, doping, and the substrate, incorrect determination is possible. A more definitive way to determine the number of layers is by comparing the interlayer shear and breathing modes (Tan et al., 2012; Zhang et al., 2013; Zhao et al., 2013b; Lee et al., 2015; Zhang et al., 2015). These vibration modes are schematically shown in Fig. 2. They are rigid vibrations of the layers along the in-plane and out-of-plane directions. Most of few-layer 2D crystals are expected to have these vibrational modes. Since these modes shift sensitively with the number of layers, they are good fingerprints of the number of layers. On the negative side, theses vibrations are located in the low-frequency region below 100 cm^{-1}, which makes it difficult to observe experimentally. A triple stage spectrometer or a single-stage spectrometer with recently developed Bragg notch filters should be used to access Raman spectra in this frequency range (Tan et al., 2012; Lee et al., 2015). The shear and breathing modes of several 2D materials have been reported (Tan et al., 2012; Zhang et al., 2013; Zhao et al., 2013b; Chen et al., 2015; Lee et al., 2015). In the case of MoS$_2$, the number of layers can be identified up to 14 layers by using

the shear and breathing modes (Lee et al., 2015).

EFFECT OF EXCITATION ENERGY

For Raman measurements of 2D materials, choosing the right excitation energy is an important factor. For example, the optical interference effect for 2D materials on SiO_2/Si substrates greatly affects the observed Raman intensity (Yoon et al., 2009b). It is well known that in order to enhance the visibility of a sample on SiO_2/Si substrates under the optical microscope (Blake et al., 2007), optimal SiO_2 thickness of 90 and 285 nm should be used. Similar interference effects also affect the Raman intensity of the 2D materials (Yoon et al., 2009b; Li et al., 2012). For thicker samples, the optimal laser wavelength depends on both the thickness of the sample and that of the SiO_2 layer on the substrate.

When the excitation energy matches an allowed optical transition energy, resonance Raman scattering occurs. Fig. 3 shows the effect of resonance on the Raman spectrum of MoS_2. In semiconducting TMDCs, complicated excitonic structures have been expected due to reduced dielectric screening of Coulomb interactions in 2D crystals (Qiu et al., 2013; Klots et al., 2014). Due to extremely large exciton binding energies, resonances with such exciton states exhibit several anomalous behaviors as reported by several groups (Chakraborty et al., 2013; Fan et al., 2014; Gołasa et al., 2014; Carvalho et al., 2015; Lee et al., 2015; Livneh et al., 2015; Pimenta et al., 2015). When the excitation energy matches the A or B exciton state, many second order Raman peaks are enhanced due to resonance with the exciton state. These second order peaks have been assigned to combinations of two phonon modes at the zone boundary near the M or K point in the Brillouin zone (Fan et al., 2014; Gołasa et al., 2014; Lee et al., 2015). However, still several peaks remain unassigned and the exact mechanism of such enhancement is not clearly understood yet. Further theoretical and experimental studies are needed. In MoS_2, the broad peak centered at the Rayleigh scattered laser line appears when a laser (1.96 eV) that matches the exciton energy is used, due to resonance excitation of the exciton states mediated by acoustic phonon scattering (Lee et al., 2015). This peak appears broader and stronger for single-layer MoS_2, which suggests that the inhomogeneity due to substrate is more pronounced in single-layer MoS_2. The intensities of the main E_{2g}^1 and A_{1g} modes also change with the excitation energy. In MoS_2, the A_{1g} mode is enhanced when the excitation energy matches the A and B exciton states (Scheuschner et al., 2012; Carvalho et al., 2015). However the E_{2g}^1 mode shows a different behavior. The E_{2g}^1 mode is relatively enhanced at a higher excitation energy of 2.81 eV, which is close to the C exciton state in MoS_2 (Qiu et al., 2013; Klots et al., 2014). The selective enhancement of the E_{2g}^1 mode with respect to the A_{1g} mode has been explained by symmetry dependent exciton-phonon coupling (Carvalho et al., 2015). In the case of WSe_2, different resonance behaviors for first- and second-order Raman modes are reported (del Corro et al., 2014). The first-order Raman modes are only weakly enhanced at resonance with the B exciton state but are strongly enhanced at resonance with A′ and B′ excited exciton states. Second-order Raman modes are enhanced at resonance with both B exciton and the excited exciton states in contrast to first-order Raman modes. This difference has been attributed to different electron-phonon coupling (del Corro et al., 2014).

EFFECTS OF STRAIN, DOPING, AND DEFECT

In addition to determination of the number of layers, Raman spectroscopy has been used to probe other basic characteristics of graphene such as defects (Dresselhaus et al., 2010; Cançado et al., 2011; Eckmann et al., 2012), strain (Mohiuddin et al., 2009; Yoon et al., 2011), and doping (Yan et al., 2007; Lee et al., 2012). Furthermore, the crystallographic orientation can be determined by measuring the polarization dependence of the Raman spectrum with the sample under uniaxial strain (Mohiuddin et al., 2009; Yoon et al., 2011; Jegal et al., 2013).

For MoS_2, several groups have reported Raman measurements under uniaxial strain (Conley et al., 2013; Wang et al., 2013). The in-plane E_{2g}^1 mode splits and redshifts whereas the out-of-plane A_{1g} mode is not affected by uniaxial strain. As in the case of graphene, the split E_{2g}^1 modes exhibit orthogonal polarization behaviors. From the polarization dependence of the split E_{2g}^1 modes, the crystallographic orientation with respect to the strain axis can be determined (Wang et al., 2013). The A_{1g} mode of MoS_2 is sensitive to doping. When a gate voltage is applied to induce electron doping in MoS_2, redshift and broadening of the A_{1g} mode are observed whereas the E_{2g}^1 mode is not affected (Chakraborty et al., 2012). This is due to stronger electron-phonon coupling of the A_{1g} mode.
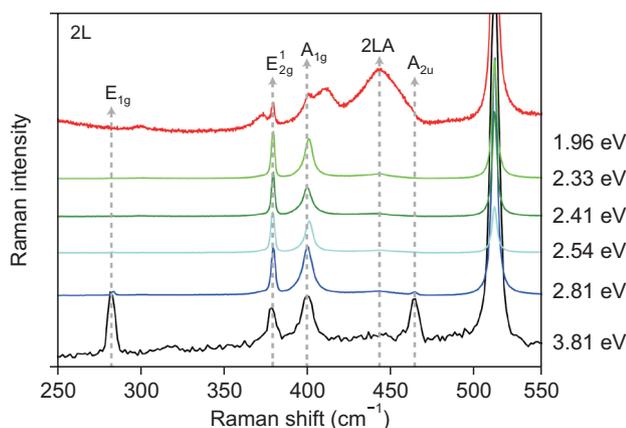

Fig. 3. Raman spectra of 2-layer MoS_2 measured with 6 excitation energies.

Therefore, the A_{1g} mode can be used to probe the effect of doping in MoS_2 (Chakraborty et al., 2012). Furthermore, the density of defects in MoS_2 can be estimated through Raman spectroscopy (Mignuzzi et al., 2015). By comparing the Raman spectra of ion bombarded MoS_2 samples with that of pristine samples, the effect of disorder on the Raman spectrum was investigated (Mignuzzi et al., 2015). Both the evolution of the linewidths and the frequency shift of the main first-order Raman modes with increasing density of defects are explained in terms of the phonon confinement model. Several peaks corresponding to zone boundary phonons are activated as the density of defects increases. The LA(M) mode at ~227 cm^{-1} is most pronounced, and its relative intensity with respect to the first-order Raman modes is proportional to the density of defects. Therefore, quantitative estimation of the density of defects is possible by using the intensity of LA(M) mode as the D peak intensity is used to estimate the degree of disorder in graphene.

SUMMARY

Raman spectroscopy in 2D materials research has much wider applications than in most other materials. In addition to structural properties, electrical properties and band structures affect the measured Raman spectrum of most 2D materials. By analyzing Raman spectra, one can obtain information on the number of layers, stacking orders, defects, crystallographic orientation, doping density, etc. In TMDCs, resonance with excitonic states results in anomalous effects, which reflect the peculiar nature of 2D materials.

CONFLICT OF INTEREST

No potential conflict of interest relevant to this article was reported.

REFERENCES

Blake P, Hill E W, Castro Neto A H, Novoselov K S, Jiang D, Yang R, Booth T J, and Geim A K (2007) Making graphene visible. *Appl. Phys. Lett.* **91**, 063124.

Cançado L G, Jorio A, Ferreira E H M, Stavale F, Achete C A, Capaz R B, Moutinho M V O, Lombardo A, Kulmala T S, and Ferrari A C (2011) Quantifying defects in graphene via Raman spectroscopy at different excitation energies. *Nano Lett.* **11**, 3190-3196.

Carvalho B R, Malard L M, Alves J M, Fantini C, and Pimenta M A (2015) Symmetry-dependent exciton-phonon coupling in 2D and bulk MoS_2 observed by resonance Raman scattering. *Phys. Rev. Lett.* **114**, 136403.

Castro Neto A H, Guinea F, Peres N M R, Novoselov K S, and Geim A K (2009) The electronic properties of graphene. *Rev. Mod. Phys.* **81**, 109-162.

Chakraborty B, Bera A, Muthu D V S, Bhowmick S, Waghmare U V, and Sood A K (2012) Symmetry-dependent phonon renormalization in monolayer MoS_2 transistor. *Phys. Rev. B* **85**, 161403.

Chakraborty B, Matte H S S R, Sood A K, and Rao C N R (2013) Layer-dependent resonant Raman scattering of a few layer MoS_2. *J. Raman Spectrosc.* **44**, 92-96.

Chen S Y, Zheng C, Fuhrer M S, and Yan J (2015) Helicity-resolved Raman scattering of MoS_2, $MoSe_2$, WS_2, and WSe_2 atomic layers. *Nano Lett.* **15**, 2526-2532.

Cong C, Yu T, Sato K, Shang J, Saito R, Dresselhaus G F, and Dresselhaus M S (2011) Raman characterization of ABA- and ABC-stacked trilayer graphene. *ACS Nano* **5**, 8760-8768.

Conley H J, Wang B, Ziegler J I, Haglund R F, Pantelides S T, and Bolotin K I (2013) Bandgap engineering of strained monolayer and bilayer MoS_2. *Nano Lett.* **13**, 3626-3630.

Dean C R, Young A F, Meric I, Lee C, Wang L, Sorgenfrei S, Watanabe K, Taniguchi T, Kim P, Shepard K L, and Hone J (2010) Boron nitride substrates for high-quality graphene electronics. *Nat. Nanotechnol.* **5**, 722-726.

del Corro E, Terrones H, Elias A, Fantini C, Feng S, Nguyen M A, Mallouk T E, Terrones M, and Pimenta M A (2014) Excited excitonic states in 1L, 2L, 3L, and bulk WSe_2 observed by resonant Raman spectroscopy. *ACS Nano* **8**, 9629-9635.

Dresselhaus M S, Jorio A, Souza Filho A G, and Saito R (2010) Defect characterization in graphene and carbon nanotubes using Raman spectroscopy. *Philos. Trans. R. Soc. A Math. Phys. Eng. Sci.* **368**, 5355-5377.

Eckmann A, Felten A, Mishchenko A, Britnell L, Krupke R, Novoselov K S, and Casiraghi C (2012) Probing the nature of defects in graphene by Raman spectroscopy. *Nano Lett.* **12**, 3925-3930.

Fan J H, Gao P, Zhang A M, Zhu B R, Zeng H L, Cui X D, He R, and Zhang Q M (2014) Resonance Raman scattering in bulk 2H-MX2 (M = Mo, W; X = S, Se) and monolayer MoS_2. *J. Appl. Phys.* **115**, 053527.

Ferrari A C and Basko D M (2013) Raman spectroscopy as a versatile tool for studying the properties of graphene. *Nat. Nanotechnol.* **8**, 235-246.

Ferrari A C, Meyer J C, Scardaci V, Casiraghi C, Lazzeri M, Mauri F, Piscanec S, Jiang D, Novoselov K S, Roth S, and Geim A K (2006) Raman spectrum of graphene and graphene layers. *Phys. Rev. Lett.* **97**, 187401.

Geim A K and Novoselov K S (2007) The rise of graphene. *Nat. Mater.* **6**, 183-191.

Gołasa K, Grzeszczyk M, Leszczyński P, Faugeras C, Nicolet A A L, Wysmołek A, Potemski M, and Babiński A (2014) Multiphonon resonant Raman scattering in MoS_2. *Appl. Phys. Lett.* **104**, 092106.

Jegal S, Hao Y, Yoon D, Ruoff R S, Yun H, Lee S W, and Cheong H (2013) Crystallographic orientation of early domains in CVD graphene studied by Raman spectroscopy. *Chem. Phys. Lett.* **568-569**, 146-150.

Klots A R, Newaz A K M, Wang B, Prasai D, Krzyzanowska H, Lin J, Caudel D, Ghimire N J, Yan J, Ivanov B L, Velizhanin K A, Burger A, Mandrus D G, Tolk N H, Pantelides S T, and Bolotin K I (2014) Probing

excitonic states in suspended two-dimensional semiconductors by photocurrent spectroscopy. *Sci. Rep.* **4**, 6608.

Lee C, Yan H, Brus L E, Heinz T F, Hone J, and Ryu S (2010) Anomalous lattice vibrations of single- and few-layer MoS$_2$. *ACS Nano* **4**, 2695-2700.

Lee J E, Ahn G, Shim J, Lee Y S, and Ryu S (2012) Optical separation of mechanical strain from charge doping in graphene. *Nat. Commun.* **3**, 1024.

Lee J U, Park J, Son Y W, and Cheong H (2015) Anomalous excitonic resonance Raman effects in few-layered MoS$_2$. *Nanoscale* **7**, 3229-3236.

Li L, Yu Y, Ye G J, Ge Q, Ou X, Wu H, Feng D, Chen X H, and Zhang Y (2014) Black phosphorus field-effect transistors. *Nat. Nanotechnol.* **9**, 372-377.

Li S L, Miyazaki H, Song H, Kuramochi H, Nakaharai S, and Tsukagoshi K (2012) Quantitative Raman spectrum and reliable thickness identification for atomic layers on insulating substrates. *ACS Nano* **6**, 7381-7388.

Liu H, Neal A T, Zhu Z, Luo Z, Xu X, Tománek D, and Ye P D (2014) Phosphorene: an unexplored 2D semiconductor with a high hole mobility. *ACS Nano* **8**, 4033-4041.

Livneh T and Spanier J E (2015) A comprehensive multiphonon spectral analysis in MoS$_2$. *2D Mater.* **2**, 035003.

Lui C H, Li Z, Chen Z, Klimov P V, Brus L E, and Heinz T F (2011) Imaging stacking order in few-layer graphene. *Nano Lett.* **11**, 164-169.

Luo X, Zhao Y, Zhang J, Toh M, Kloc C, Xiong Q, and Quek S Y (2013) Effects of lower symmetry and dimensionality on Raman spectra in two-dimensional WSe$_2$. *Phys. Rev. B* **88**, 195313.

Mak K F, Lee C, Hone J, Shan J, and Heinz T F (2010) Atomically thin MoS$_2$: a new direct-gap semiconductor. *Phys. Rev. Lett.* **105**, 136805.

Mignuzzi S, Pollard A J, Bonini N, Brennan B, Gilmore I S, Pimenta M A, Richards D, and Roy D (2015) Effect of disorder on Raman scattering of single-layer MoS$_2$. *Phys. Rev. B* **91**, 195411.

Mohiuddin T M G, Lombardo A, Nair R R, Bonetti A, Savini G, Jalil R, Bonini N, Basko D M, Galiotis C, Marzari N, Novoselov K S, Geim A K, and Ferrari A C (2009) Uniaxial strain in graphene by Raman spectroscopy: G peak splitting, Grüneisen parameters, and sample orientation. *Phys. Rev. B* **79**, 205433.

Molina-Sánchez A and Wirtz L (2011) Phonons in single-layer and few-layer MoS$_2$ and WS$_2$. *Phys. Rev. B* **84**, 155413.

Nguyen T A, Lee J U, Yoon D, and Cheong H (2014) Excitation energy dependent Raman signatures of ABA- and ABC-stacked few-layer graphene. *Sci. Rep.* **4**, 4630.

Novoselov K S, Geim A K, Morozov S V, Jiang D, Zhang Y, Dubonos S V, Grigorieva I V, and Firsov A A (2004) Electric field effect in atomically thin carbon films. *Science* **306**, 666-669.

Pimenta M A, del Corro E, Carvalho B R, Fantini C, and Malard L M (2015) Comparative study of Raman spectroscopy in graphene and MoS$_2$-type transition metal dichalcogenides. *Acc. Chem. Res.* **48**, 41-47.

Qiu D Y, da Jornada F H, and Louie S G (2013) Optical spectrum of MoS$_2$: many-body effects and diversity of exciton states. *Phys. Rev. Lett.* **111**, 216805.

Scheuschner N, Ochedowski O, Schleberger M, and Maultzsch J (2012) Resonant Raman profiles and µ-photoluminescence of atomically thin layers of molybdenum disulfide. *Phys. Status Solidi* **249**, 2644-2647.

Staiger M, Gillen R, Scheuschner N, Ochedowski O, Kampmann F, Schleberger M, Thomsen C, and Maultzsch J (2015) Splitting of monolayer out-of-plane A$_1'$ Raman mode in few-layer WS$_2$. *Phys. Rev. B* **91**, 195419.

Tan P H, Han W P, Zhao W J, Wu Z H, Chang K, Wang H, Wang Y F, Bonini N, Marzari N, Pugno N, Savini G, Lombardo A, and Ferrari A C (2012) The shear mode of multilayer graphene. *Nat. Mater.* **11**, 294-300.

Tonndorf P, Schmidt R, Böttger P, Zhang X, Börner J, Liebig A, Albrecht M, Kloc C, Gordan O, Zahn D R T, Michaelis de Vasconcellos S, and Bratschitsch R (2013) Photoluminescence emission and Raman response of monolayer MoS$_2$, MoSe$_2$, and WSe$_2$. *Opt. Express* **21**, 4908-4916.

Wang Q H, Kalantar-Zadeh K, Kis A, Coleman J N, and Strano M S (2012) Electronics and optoelectronics of two-dimensional transition metal dichalcogenides. *Nat. Nanotechnol.* **7**, 699-712.

Wang Y, Cong C, Qiu C, and Yu T (2013) Raman spectroscopy study of lattice vibration and crystallographic orientation of monolayer MoS$_2$ under uniaxial strain. *Small* **9**, 2857-2861.

Yan J, Zhang Y, Kim P, and Pinczuk A (2007) Electric field effect tuning of electron-phonon coupling in graphene. *Phys. Rev. Lett.* **98**, 166802.

Yoon D, Moon H, Cheong H, Choi J, Choi J, and Park B (2009a) Variations in the Raman spectrum as a function of the number of graphene layers. *J. Korean Phys. Soc.* **55**, 1299-1303.

Yoon D, Moon H, Son Y W, Choi J S, Park B H, Cha Y H, Kim Y D, and Cheong H (2009b) Interference effect on Raman spectrum of graphene on SiO$_2$/Si. *Phys. Rev. B* **80**, 125422.

Yoon D, Son Y W, and Cheong H (2011) Strain-dependent splitting of the double-resonance raman scattering band in graphene. *Phys. Rev. Lett.* **106**, 155502.

Zhang X, Han W P, Wu J B, Milana S, Lu Y, Li Q Q, Ferrari A C, and Tan P H (2013) Raman spectroscopy of shear and layer breathing modes in multilayer MoS$_2$. *Phys. Rev. B* **87**, 115413.

Zhang X, Qiao X F, Shi W, Wu J B, Jiang D S, and Tan P H (2015) Phonon and Raman scattering of two-dimensional transition metal dichalcogenides from monolayer, multilayer to bulk material. *Chem. Soc. Rev.* **44**, 2757-2785.

Zhao W, Ghorannevis Z, Amara K K, Pang J R, Toh M, Zhang X, Kloc C, Tan P H, and Eda G (2013a) Lattice dynamics in mono- and few-layer sheets of WS$_2$ and WSe$_2$. *Nanoscale* **5**, 9677.

Zhao Y, Luo X, Li H, Zhang J, Araujo P T, Gan C K, Wu J, Zhang H, Quek S Y, Dresselhaus M S, and Xiong Q (2013b) Interlayer breathing and shear modes in few-trilayer MoS$_2$ and WSe$_2$. *Nano Lett.* **13**, 1007-1015.